

Study of Rock-Lining Interaction for Circular Tunnels Using Finite Element Analysis

A. A. Elsayed

Modern Academy for Engineering and Technology, Cairo, Egypt

ABSTRACT

Finite element technique is used to model two phases of tunneling process, namely; excavation and rock-lining interaction. The excavation phase is responsible for determining the pre-lining rock mass deformations and the reduced *in-situ* stresses. The interaction phase models the compatibility of the rock-lining system. The deformations and stresses of the rock-lining system and the final rock mass pressure acting on the lining are determined. The finite element results are compared with the results of the Convergence-Confinement method for the case study (Shimizu Tunnel) that was guided by field measurements.

One of the main objectives of this study is to investigate the effect of different parameters on the behavior of excavated tunnel before and after lining activation. The analysis followed the same procedure which had been applied in the analysis of the case of Shimizu Tunnel taking into consideration the different values of the tunnel radius and the depth of excavated tunnel through different qualities of rock ranging between poor, moderate and hard rock. The parametric study has been conducted for circular tunnel.

The first lining system involved in this study was assumed to be shotcrete of thicknesses of 20, 30, 40 and 50cm, and the second lining system was steel ribs with shotcrete of thicknesses of 20, 30, 40 and 50cm. The results of Finite Element Analysis were presented for different thicknesses.

KEYWORDS: Convergence-confinement approach, Rock tunnels, Ground reaction curve, Shotcrete, Support characteristics curve, Lining system.

INTRODUCTION

Realistic analysis of the tunnel behavior and lining interaction requires a full understanding for the tunneling procedure to simulate its effect in the analytical model. The ground movements due to tunneling, the lining installation and the rock-liner behavior are different elements of the mechanism which must be idealized in the analytical model. Simulation of these elements requires adequate representation of the strain-strength characteristics of the ground and some

major details of the tunneling construction process. The interaction between the rock and the lining requires input data concerning the rock and the lining materials' properties and the structural idealization of the lining in the overall system. The interface properties between the rock and the lining must be simulated in the analytical model to ensure the compatibility between the lining and the surrounding rock. Therefore, the simulation procedure of the problem goes through the following two stages:

- Excavation Phase: this phase of the analysis starts with the initial state of the stresses present in the ground up to the liner activation including ground

deformation associated with tunneling operation.

- Interaction Phase: this phase of the analysis defines the interaction behavior between the rock and the liner.

FINITE ELEMENT SIMULATION

Idealized ground profile at the Shimizu Tunnel is shown in Figure 1. Analysis of displacements and stresses around the tunnel was carried out using a 2-D plane strain finite element PLAXIS version 8.2, taking into consideration the linear-elastic behavior of the lining and the ground materials. The finite element mesh used to carry out the simulation for the excavation phase is shown in Figure 2. The mesh used for the interaction simulation phase is shown in Figure 3.

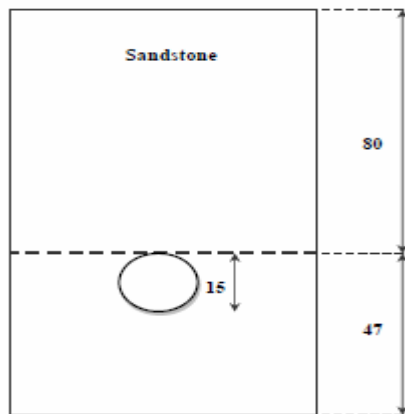


Figure 1: Ground profile for the tunnel

MATERIAL MODELS AND PROPERTIES

Ground

The linear elastic model is used for characterizing the ground material, which consists of two different layers with the following average mechanical properties as recommended by Lama and Vutukuri (1978) and Goodman (1980).

- Sandstone
 - E: Young's modulus = 487 MPa
 - ν : Poisson's ratio = 0.3
 - γ : unit weight density = 25 kN/m³

- GSI: Geological Strength Index = 40
- m_i : Intact rock parameter = 19
- σ_{ci} : Unconfined compressive strength = 75 MPa
- K_0 : Coefficient of lateral pressure = 0.83

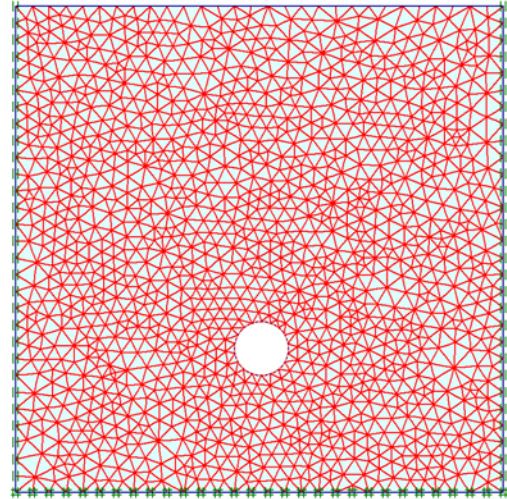


Figure 2: Finite element mesh for the excavation phase

Lining

- Shotcrete
 - E: Young's modulus = 18×10^6 MPa
 - ν : Poisson's ratio = 0.25 kN/m³
 - T_c : Shotcrete thickness = 0.2m
 - γ : unit weight density = 25 kN/m³
 - σ_{ci} : Unconfined compressive strength = 35.3 MPa
- Steel ribs
 - E: Young's modulus = 21×10^4 MPa
 - ν : Poisson's ratio = 0.25
 - γ : unit weight density = 78 kN/m³

STRUCTURAL STATIC ANALYSIS

The solution of the problem depends on a static analysis, which was used to determine the displacements, stresses, strains and forces in the ground and different lining systems caused by acting loads. These loads depend mainly on the depth of the overburden above the tunnel under the effect of initial

in-situ stresses which can be divided into vertical stresses and horizontal stresses and taking into consideration the effect of coefficient of earth pressure ($k_e=0.83$). The effect of any expected dynamic loads is neglected.

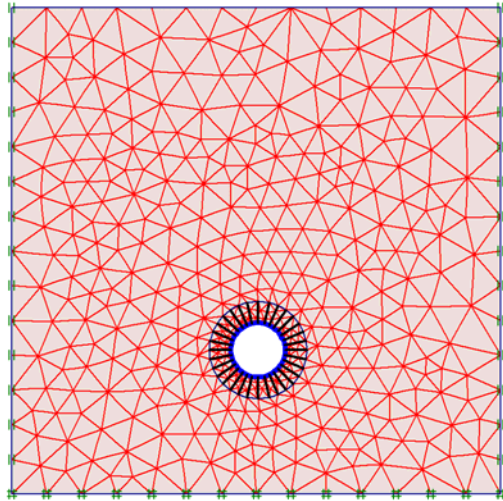


Figure 3: Finite element mesh for the interaction phase

LOADING AND BOUNDARY CONDITIONS

The total value of each force is divided into two ratios depending on the excavation and interaction phases as follows:

- 80% of each force will be applied in the excavation phase to simulate the stress releases after excavation.
- 20% of each force will be applied in the interaction phase to simulate the ground-lining interaction to achieve the state of equilibrium between ground and steel ribs lining.

In case of shotcrete with steel ribs lining, the loads will be divided into 85% for excavation phase and 15% for interaction phase because the stress releasing will be greater due to the using of a combination between two different lining types.

Boundary Conditions

A set of boundary conditions was defined for the

model to provide stability to the structural system. The analysis model was established with a fixed boundary at the bottom and roller supports on sides, such that the displacement in the x-direction at the two vertical sides of the model is equal to zero ($u_x=0$). The displacement in the y-direction at the bottom horizontal boundary of the model is equal to zero ($u_y=0$).

ANALYSIS OF SHIMIZU TUNNEL

Excavation Phase

The effect of tunnel excavation process on the vertical ground displacements' values for the whole profile of the excavated tunnel are shown in Figure 4. It is noticed that the vertical displacement (settlement) above the tunnel is increased from the ground surface down to the tunnel crown. The settlement at the tunnel crown is downward due to the downward unloading. The vertical displacement below the tunnel (heave) decreased gradually for points located at lower levels below the tunnel invert. The displacement at the tunnel invert is upward and is always smaller than the displacement at the tunnel crown due to the increasing of the ground stiffness.

The maximum value of final horizontal displacement was about 2.88 mm. It can be neglected at the crown and the invert due to the boundary of the ground mass at these locations. The horizontal displacement decreased from the tunnel surface going through ground mass.

The horizontal ground displacement adjacent to the tunnel is shown in Figure 5. The average radial displacement ahead the tunnel face is estimated as 3.43 mm along the perimeter of excavated tunnel which resulted from the releasing of stresses after excavation process. This value on the Ground Reaction Curve is estimated as 2.6mm.

The values of vertical, horizontal and radial displacements at the tunnel crown, spring line and invert of the tunnel are listed in Table 1.

Table 1: Values of displacements due to excavation

Location	Vertical displacement	Horizontal displacement	Radial displacement
Crown	4.3mm	0	4.3mm
Spring line	0.45mm	2.85mm	2.88mm
Invert	3.67mm	0	3.68mm

The vertical *in-situ* stresses around the tunnel are changed due to the excavation process. These changes are shown in Figure 6. It is obvious that the changes of stresses at the crown and the invert are tension due to

the inward movement of the ground in the vertical direction. It is downward at the crown and upward at the invert. But, at the spring line, the increase of stresses is compression because of stress arching. The increase of horizontal stresses at the crown and the invert is compression due to stress arching, and at the spring line, the change of horizontal stresses is tension due to the inward ground movement in the horizontal direction. The values of change in horizontal stresses are shown in Figure 7. The values of vertical, horizontal and the radial stresses at the crown, the spring line and the invert of the tunnel are summarized in Table 2.

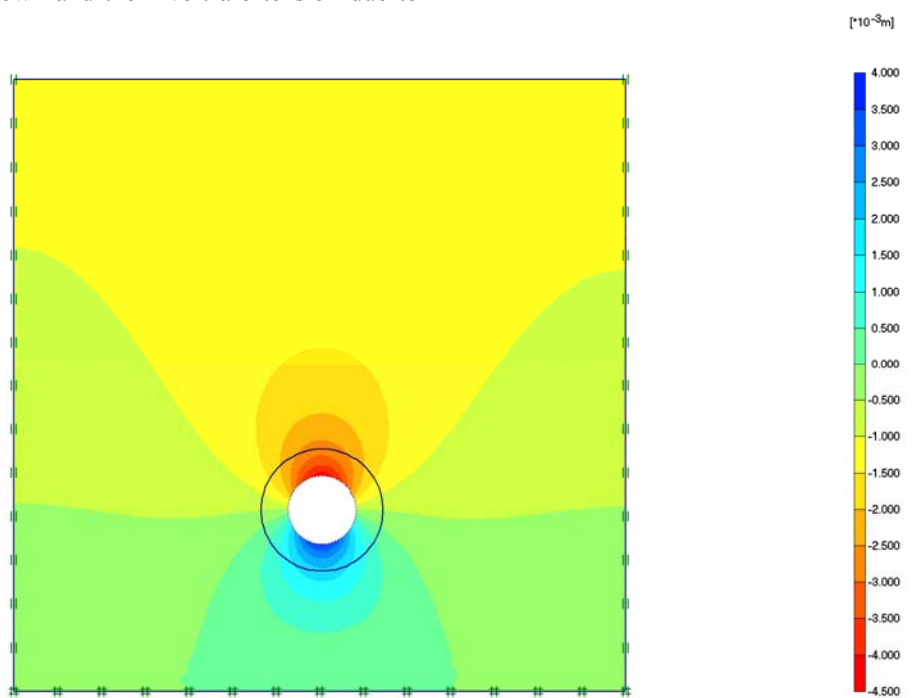


Figure 4: Vertical displacement due to tunnel excavation before lining

Rock-Lining Interaction

Evaluation of Ground Movements and Stresses Due to Shotcrete and Rock Bolts with Steel Ribs Lining

The average radial displacement for the tunnel wall at the lining phase is equal to 0.62mm, where the value on Ground Reaction Curve is equal to 1.1mm. The total average radial displacement is equal to the sum average

radial displacements of the excavation and interaction phases, which are equal to 3.43mm and 0.62mm. The resulting value is equal to 4.05mm, while the value on the Ground Reaction Curve is equal to 3.7mm. The values of final radial displacements and final radial stresses in rock mass at the tunnel crown, springline and invert are listed in Table 3. Figure 8 shows the final radial displacement.

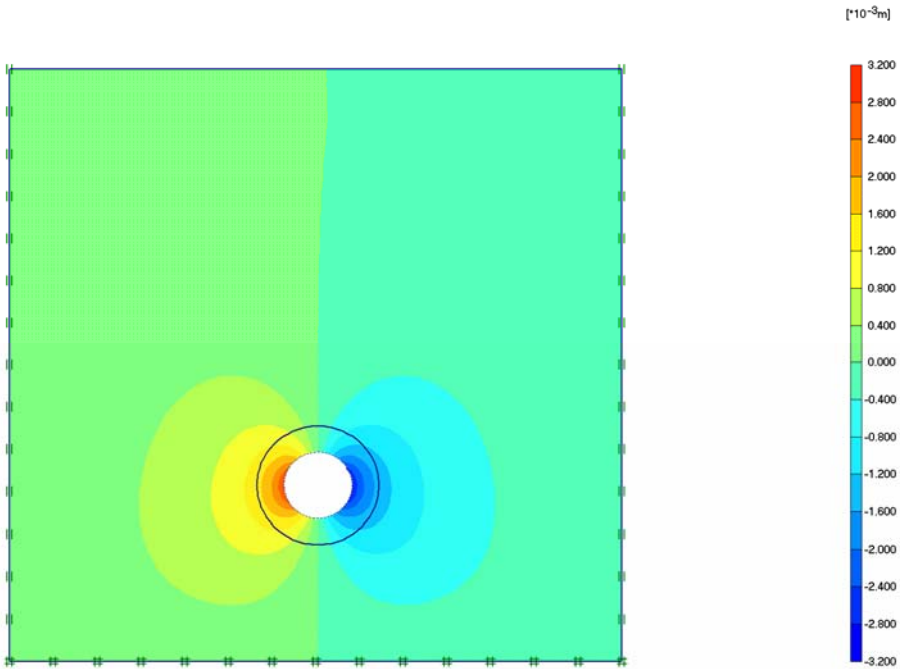


Figure 5: Horizontal displacement due to tunnel excavation before lining

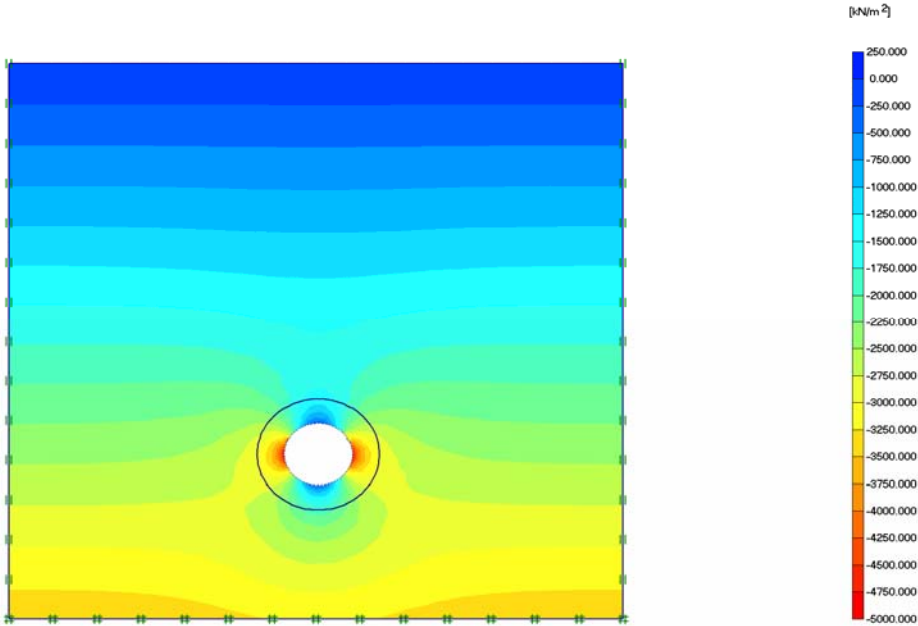


Figure 6: Vertical stresses due to tunnel excavation before lining

Table 2: Values of change in stresses due to excavation

Location	Vertical stresses	Horizontal stresses	Radial stresses
Crown	$-1.62 \times 10^3 \text{ kN/m}^2$	$-3.00 \times 10^3 \text{ kN/m}^2$	$3.40 \times 10^3 \text{ kN/m}^2$
Springline	$-4.44 \times 10^3 \text{ kN/m}^2$	$-1.96 \times 10^3 \text{ kN/m}^2$	$4.80 \times 10^3 \text{ kN/m}^2$
Invert	$-3.22 \times 10^3 \text{ kN/m}^2$	$-3.34 \times 10^3 \text{ kN/m}^2$	$4.63 \times 10^3 \text{ kN/m}^2$

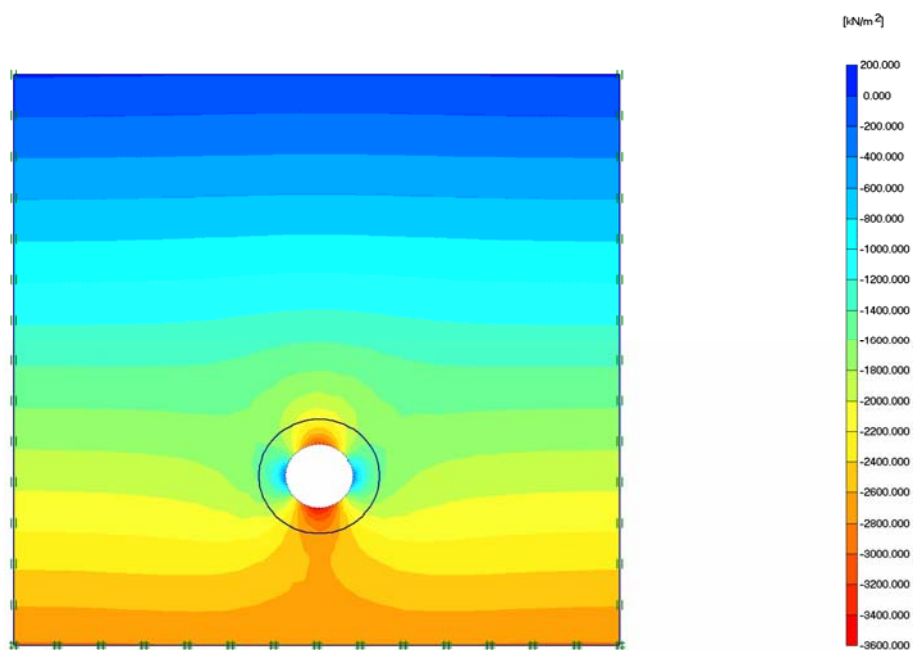


Figure 7: Horizontal stresses due to tunnel excavation before lining

Table 3: Values of final radial displacement and final radial stresses in rock mass

Location	Final radial displacement	Final radial stresses
Crown	4.38mm	$4.7 \times 10^3 \text{ kN/m}^2$
Springline	2.92mm	$6.51 \times 10^3 \text{ kN/m}^2$
Invert	3.73mm	$6.5 \times 10^3 \text{ kN/m}^2$

The final acting pressure values on the shotcrete with steel ribs lining due to 20% of the total *in-situ*

stresses at the tunnel crown, spring line and invert are presented in Table 4 and illustrated in Figure 9. Table 4 presents also the field measurements and the percentages of difference between these measurements and the results of finite element analysis. The average acting pressure on shotcrete with steel ribs lining is equal to $4.09 \times 10^3 \text{ kN/m}^2$. It should be noted that the value of released stresses in excavation phase is equal to 80% of the total *in-situ* stresses because the activation of the three lining systems (steel ribs, shotcrete and rock bolts) takes more time than the activation of steel ribs

only. Therefore, the value of average radial displacement is greater than the corresponding value in case of steel ribs lining system, but the efficiency of this system is better because its load capacity is higher. Finally, after calibration of ShimizuTunnel by the finite element analysis with the Convergence-Confinement

approach which was guided by field measurements, the results proved that the utilized finite element procedure is a good procedure for the ground-lining interaction. Hence, the finite element analysis was used for a parametric study to evaluate the effect of different parameters on rock-lining interaction.

Table 4: Final acting pressure on shotcrete and rock bolts with steel ribs lining

Location	Final acting pressure on lining		Difference (%)
	Finite Element	Field Measurements	
Crown	$3.26 \times 10^3 \text{ kN/m}^2$	$2.97 \times 10^3 \text{ kN/m}^2$	8.9 %
Springline	$4.41 \times 10^3 \text{ kN/m}^2$	$5.08 \times 10^3 \text{ kN/m}^2$	13.2 %
Invert	$4.61 \times 10^3 \text{ kN/m}^2$	$5.21 \times 10^3 \text{ kN/m}^2$	11.5 %

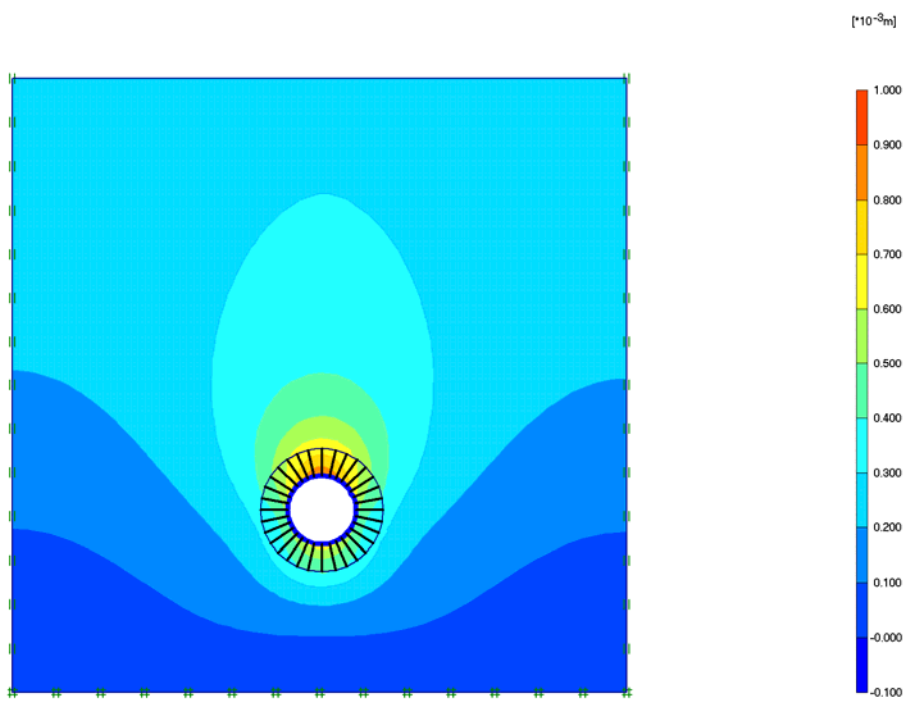


Figure 8: Final radial displacement on tunnel perimeter after shotcrete and rock bolts with steel ribs

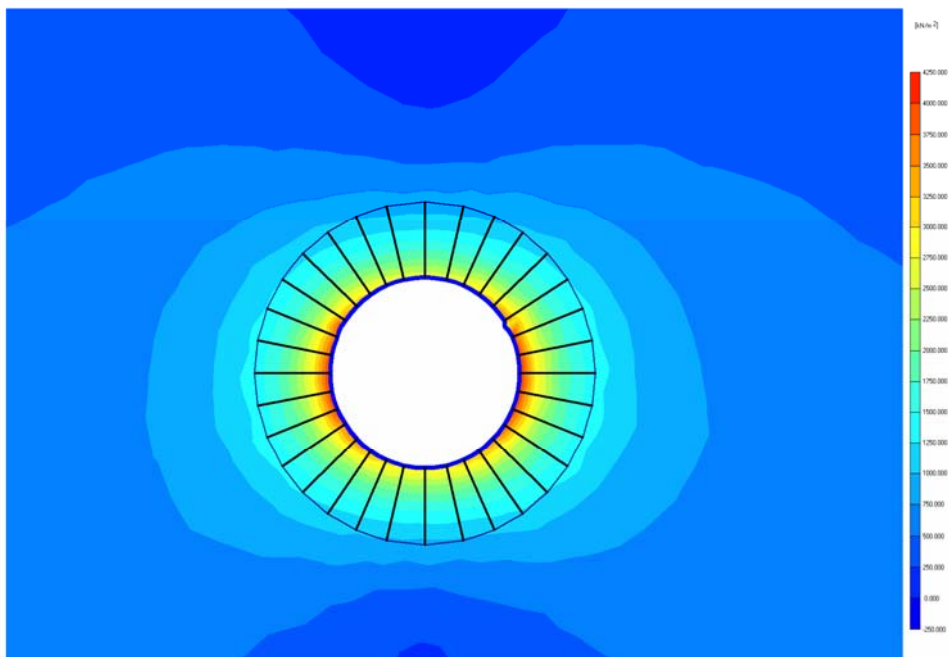


Figure 9: Final radial stresses on tunnel perimeter after shotcrete and rock bolts with steel ribs

Table 5: Results of shotcrete lining

Method	Radial displacement in rock mass	Radial displacement in lining system
Convergence Method	2.28 mm	0.48
Finite Element	1.9 mm	0.6
Difference (%)	16 %	20 %

Table 6: Results of shotcrete lining

Method	Radial displacement in rock mass	Radial displacement in lining system
Convergence Method	2.32 mm	0.3
Finite Element	1.9 7mm	0.37
Difference (%)	15 %	18 %

Table 7: Results of shotcrete lining

Method	Radial displacement in rock mass	Radial displacement in lining system
Convergence Method	6.19 mm	0.7
Finite Element	5.7mm	0.62
Difference (%)	8 %	11 %

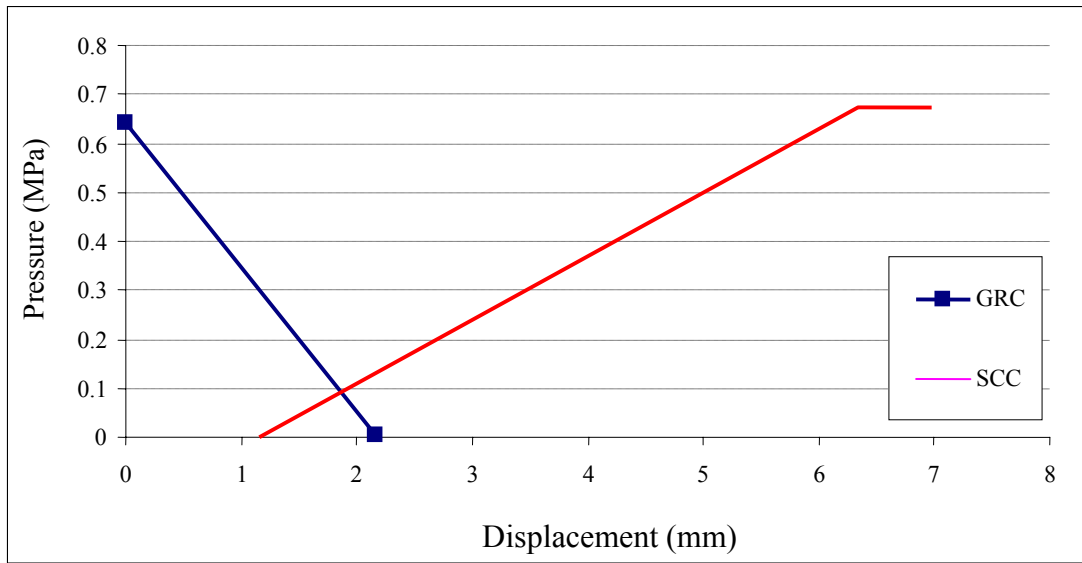


Figure 10: Support characteristic curve for shotcrete in hard rock

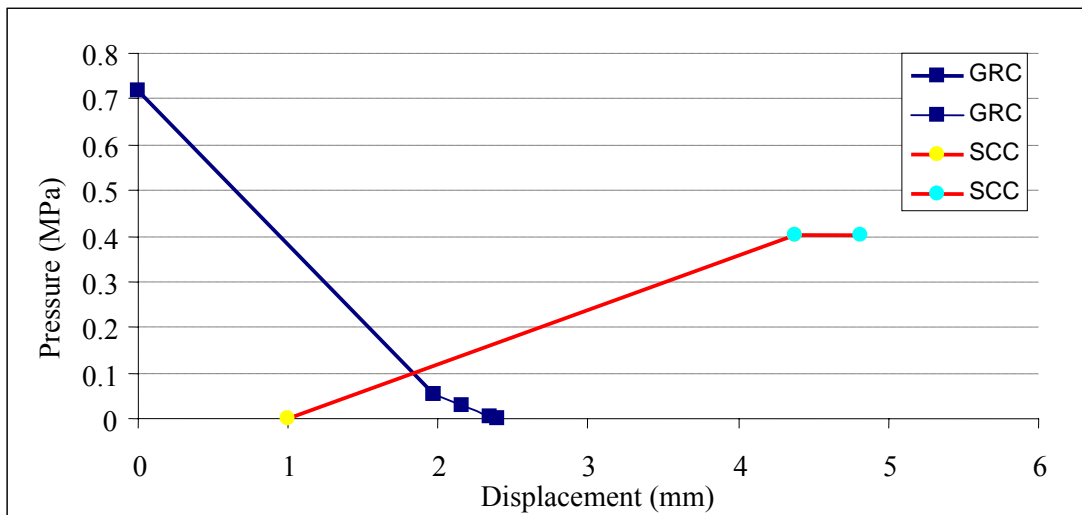


Figure 11: Support characteristic curve for shotcrete in moderate rock

CALIBRATION OF THE FINITE ELEMENT

Hard Rock

Evaluation of Ground Movements Due to Shotcrete Lining

The average radial displacement for the tunnel perimeter at the lining phase is equal to 0.42mm, where the value on the Ground Reaction Curve is equal to 0.48mm.

The total average radial displacement is equal to the

sum of the average radial displacements of the excavation and interaction phases, which are equal to 1.86mm and 0.42mm, respectively.

The resulting value is equal to 2.28mm, while the value on the Ground Reaction Curve is equal to 1.9 mm. Figure 10 shows the support characteristic curve for shotcrete in hard rock. It is clear that the resulting values of the two analysis procedures are compatible. The results of the finite element analysis with the convergence-

confinement approach, for the used coefficient of lateral

pressure (k_0) of 1, are presented in Table (5).

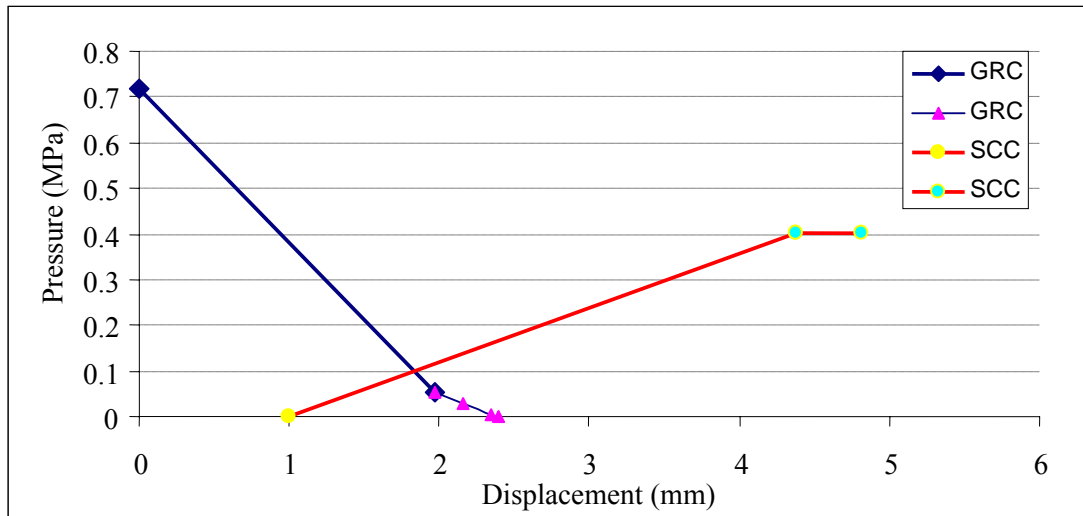


Figure 12: Support characteristic curve for shotcrete in poor rock

Moderate Rock

Evaluation of Ground Movements Due to Shotcrete Lining

The average radial displacement for the tunnel perimeter at the lining phase is equal to 0.26mm, where the value on the Ground Reaction Curve is equal to 0.3mm.

The total average radial displacement is equal to the sum of the average radial displacements of the excavation and interaction phases, which are equal to 2.06mm and 0.26mm, respectively. The resulting value is equal to 2.32 mm, while the value on the Ground Reaction Curve is equal to 1.97 mm. Figure 11 shows the support characteristic curve for shotcrete in moderate rock. It is clear that the resulting values of the two analysis procedures are compatible. The results of the finite element analysis with the convergence-confinement approach, for the used coefficient of lateral pressure (k_0) of 1, are presented in Table (6).

Poor Rock

Evaluation of Ground Movements Due to Shotcrete Lining

The average radial displacement for the tunnel

perimeter at the lining phase is equal to 0.51mm, where the value on the Ground Reaction Curve is equal to 0.7mm. The total average radial displacement is equal to the sum of the average radial displacements of the excavation and interaction phases, which are equal to 5.68mm and 0.51mm, respectively. The resulting value is equal to 6.19 mm, while the value on the Ground Reaction Curve is equal to 5.7mm. Figure 12 shows the support characteristic curve for shotcrete in poor rock. It is clear that the resulting values of the two analysis procedures are compatible. The results of the finite element analysis with the convergence-confinement approach, for the used coefficient of lateral pressure (k_0) of 1, are presented in Table (7).

PARAMETRIC STUDY

One of the main objectives of this study was to investigate the effect of different parameters on the behavior of excavated tunnel before and after lining activation. The analysis followed the same procedure which had been applied in the analysis of the case of Shimizu Tunnel, taking into consideration the different values of the tunnel radius and the depth of excavated

tunnel through different qualities of rock ranging between poor, moderate and hard rock. The parametric

study has been conducted for circular tunnel as follows:

- Circular tunnel

$$R_1 = 3 \text{ m}$$

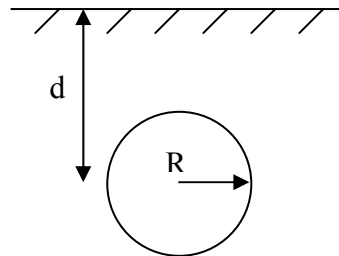
$$d_1 = 10 \text{ m}$$

$$R_2 = 4.5 \text{ m}$$

$$d_2 = 20 \text{ m}$$

$$R_3 = 6 \text{ m}$$

$$d_3 = 30 \text{ m}$$



The depth of the tunnel (d) is measured from ground surface to the center line of the tunnel. Table 8 contains the geotechnical properties of different rock mass qualities which are used for the parametric study. The purpose of this study is to display the effect of different parameters, such as: the dimensions of the tunnel, Young's modulus (E), depth of the overburden above the

tunnel center line (d), shear modulus (G) and unconfined compressive strength (σ_{ci}) on the displacements of the ground and the lining and the final load of the lining. The geotechnical properties of hard, moderate and poor rock were obtained from Lama and Vutukuri (1978) and Goodman (1980).

Table 8: Geotechnical properties of different rock mass qualities

Type of rock	σ_{ci} MPa	GSI	ν	E_{rm} MPa	G MPa	γ kN/m ³
Poor rock	10	25	0.2	1000	0.312	24
Mod. rock	25	35	0.25	30×10^3	0.843	24.1
Hard rock	73	40	0.38	18.3×10^3	0.738	21.4

where:

σ_{ci} : unconfined compressive strength.

GSI: Geotechnical Strength Index.

ν : Poisson's ratio.

E_{rm} : Young's modulus of rock mass.

G: Shear modulus.

γ : Unit weight.

The total value of each force is divided into two ratios depending on the excavation and interaction phases as follows:

- 80% of each force will be applied in the excavation phase to simulate the stress releases after excavation.

- 20% of each force will be applied in the interaction phase to simulate the ground-lining interaction to achieve the state of equilibrium between rock and shotcrete with steel ribs lining.

The changes of average radial displacement and radial stresses are the major aim of the obtained results for each model analysis. The analysis consists of 18 models for circular tunnel before lining activation for poor, moderate and hard rock. Also, the analysis consists of three models for circular shape with a diameter $D=12$ m at a depth equal to 50 m excavated through poor, moderate and hard rock to be lined with shotcrete with steel ribs lining system. The results for

different circular tunnel cases before and after lining activation are shown in Tables (9-12).

Table 9: Finite Element results of different circular tunnel cases due to tunnel excavation

Tunnel condition	R (m)	d (m)	Average radial displacement in rock mass (mm)	Average radial displacement in lining system (mm)	Final (mm)
Poor rock	3	10	1.14	0.09	1.23
		20	1.93	0.15	2.08
		30	2.08	0.22	2.3
	4.5	10	1.91	0.21	2.12
		20	3.04	0.32	3.36
		30	4.31	0.45	4.76
	6	10	2.79	0.37	3.16
		20	4.42	0.45	4.87
		30	6.1	0.50	6.6
Moderate rock	3	10	0.41	0.05	0.46
		20	0.7	0.1	0.8
		30	1.2	0.11	1.31
	4.5	10	0.69	0.11	0.8
		20	1.12	0.18	1.3
		30	1.59	0.26	1.85
	6	10	1.01	0.17	1.18
		20	1.64	0.3	1.94
		30	2.25	0.33	2.58
Hard rock	3	10	0.41	0.056	0.47
		20	0.72	0.09	0.81
		30	1.04	0.11	1.15
	4.5	10	0.68	0.11	0.79
		20	1.07	0.17	1.24
		30	1.55	0.25	1.8
	6	10	0.98	0.17	1.15
		20	1.67	0.29	1.96
		30	2.29	0.4	2.69

Table 10: Finite element results of circular tunnel (D=12m, d=50m) in poor rock

Tunnel condition	Average radial displacement (mm)	Average radial pressure due to lining activation (kPa)
Before lining activation	9.9	Not applicable
After lining activation	0.32	112.2
Final	10.22	112.2

Table 11: Finite element results of circular tunnel (D=12m, d=50m) in moderate rock

Tunnel condition	Average radial displacement (mm)	Average radial pressure due to lining activation (kPa)
Before lining activation	3.66	Not applicable
After lining activation	0.25	109.5
Final	3.9	109.5

Table 12: Finite element results of circular tunnel (D=12m, d=50m) in hard rock

Tunnel condition	Average radial displacement (mm)	Average radial pressure due to lining activation (kPa)
Before lining activation	3.5	Not applicable
After lining activation	0.3	97.1
Final	3.8	97.1

Table 13: Results of shotcrete lining system

Shotcrete thick. (cm)	Average displacement in rock mass	Average displacement in lining system (mm)
20	4.39	0.59
30	4.20	0.47
40	4.04	0.33
50	3.87	0.23

Table 14: Results of shotcrete with steel ribs lining system

Shotcrete thick. with steel ribs (cm)	Average displacement in rock mass (mm)	Average displacement in lining system (mm)
20	4.25	0.47
30	4.11	0.38
40	3.99	0.27
50	3.77	0.18

Rock-lining Interaction

The first lining system involved in this study was assumed to be shotcrete of thicknesses of 20, 30, 40 and 50cm, and the second lining system was steel ribs with shotcrete of thicknesses of 20, 30, 40 and 50 cm.

The results of Finite Element Analysis for different thicknesses of shotcrete of 20, 30, 40 and 50cm are listed in Table 13.

The results of Finite Element Analysis for different thicknesses of shotcrete of 20, 30, 40 and 50cm with steel ribs are listed in Table 14.

CONCLUSIONS

- Results of the interaction of the sandstone rock with different lining systems were similar with those obtained from field measurements of the Convergence-Confinement approach.
- Results of the parametric study indicated that the greater the value of the modulus of elasticity (E),

the lower the value of average radial displacement. So, the value of average radial displacement in case of moderate rock is nearly half its value in case of poor rock due to that the value of Young's modulus for moderate rock is twice its value in case of poor rock.

- For the lining of shotcrete with thicknesses of 20, 30, 40 and 50 cm, the average displacement is equal to 4.39, 4.2, 4.04 and 3.87mm, respectively.
- For the lining of shotcrete with steel ribs with thicknesses of 20, 30, 40 and 50 cm, the average displacement is equal to 4.25, 4.11, 3.99 and 3.77mm, respectively. Therefore, the lining of shotcrete with steel ribs reduces the displacement by 9.7% than the lining of shotcrete.
- For a circular tunnel with a diameter up to 12 m excavated through poor rock, shotcrete with steel ribs lining system is essential for supporting the tunnel.

REFERENCES

- Abu-Krishna, A. 2001. Settlement Control of CWO Sewer Tunnel During Boring El-Azhar Road Tunnel in Cairo, Proc. of the International World Congress, Milano, 10-13 June.
- Amadei, B. and Tonona, F. 2003. Stresses in Anisotropic Rock Masses: An Engineering Perspective Building on Geological Knowledge, *International Journal of Rock Mechanics and Mining Sciences*.
- Bieniawski, Z. T. 1976. Rock Mass Classification in Rock Engineering, in: Bieniawski (Ed.), Proc. of Symp. on Exploration for Rock Engineering, Cape Town, Rotterdam, Balkema.
- Carranza-Torres, C. and Fairhurst, C. 2000. Application of the Convergence-Confinement Method of Tunnel Design to Rock Masses That Satisfy the Hoek-Brown Failure Criterion, *Magazine of Tunneling and Underground Space Technology*, 15 (2), Published by Elsevier Science, Ltd., 2000.
- Criag, R.N. and Muir Wood. 1978. A New Review of Tunnel Lining Practice in the United Kingdom, Transport and Road Research Laboratory Supplementary, Report 335, TRRL, Crowthorne, UK. Quoted from Muir Wood, 2000.
- Hoek, E. and Brown, T. Underground Excavation in Rock, London, The Institute of Mining and Metallurgy, Quoted from Carranza-Torres, C. and Fairhurst, C., *Magazine of Tunneling and Underground Space Technology*, 15 (2), Published by Elsevier Science, Ltd., 2000.
- Lama and Vutukuri. 1978. and Goodman. 1980. Engineering Properties of Soil and Rock.
- Panet, M. 1995. Calculdes Tunnel Par Method de Convergence-Confinement, Paris Press de l'ecole National Deponts et Chaussees, Quoted from Carranza-Torres, C. and Fairhurst, C., *Magazine of Tunneling and Underground Space Technology*, 15 (2), Published

- by Elsevier Science, Ltd., 2000.
- Panet, M. and Guenot, A. 1982. Analysis of Convergence behind the Face of a Tunnel, Institute of Mining and Metallurgy, London.
- Rabcewicz, L.V. 1964. The New Austrian Tunneling Method, Water Power.
- Sabatini, P. J., Bacchus, R.C., Mayne, P.W. and Schneider, J.A. 2002. Evaluation of Soil and Rock properties, April.
- Serafim, J. L. and J. P. Pereira. 1983. Consideration of the Geotechnical Classification of Bieniawski, in: Proc. Int. Symp on Engineering Geology and Underground Construction, Lisbon, 1 (II), 33-44, Quoted from Carranza-Torres, C. and Fairhurst, C., *Magazine of Tunneling and Underground Space Technology*, 15, (2), Published by Elsevier Science, Ltd., 2000.
- Stephenson, O. 1999. Underground Chambers in Hard Rock Masses, Quoted from Bell, F.G., Engineering in Rock Mechanics, Butterworth-Heinemann, Ltd., 443.
- Terzaghi, K. 1964. An Introduction to Tunnel Geology in Rock Tunneling with Steel Supports, by Proctor, R. V. and White, T. L. The Commercial Shearing and Stamping Co., Youngstown, Ohio, U. S. A.
- Thomson, S. and El-Nahhas, F. 1980. Field Measurements in Two Tunnels in Edmonton, Alberta, *Canadian Geotechnical Journal*, 17 (1): 20-33.